Journal of the Korea Institute of Applied Superconductivity and Cryogenics
Vol.10, No.4, (2008), pp.33~37

Study on Pressure drop characteristics in HTS cable core with two flow passages

Junkyoung Lee[1,*], Seokho Kim[2], Haejoon Kim[2], Jeonwook Cho[2]

[1]Kyungnam University, Masan 631-701, Republic of Korea
[2]Korea Electrotechnology Research Institute, Changwon, Kyungnam 641-120, Republic of Korea

***Abstract*— The main objective of this study is to identify the pressure drop characteristics of coolant flow passages of 154kV/1GVA High Temperature Superconducting (HTS) power cable, experimentally. The passages were consisted of two parts, the one is the circular path with spiral ribs in the core to cool the cable conductor layer and the other is annular path with spirally corrugated outer wall to cool the shield layer. Thus the experiments to acquire the pressure drop data were performed with two types of circular spiral tubes and eight types of the concentric annuli in various range of Reynolds number. The pressure drops in the core tubes and the annuli were much higher than those in the tubes with smooth surface. Therefore, modified correlations to present the experimental results in each flow passage were suggested.**

1. INTRODUCTION

High Temperature Superconducting (HTS) cable is emerging as a solution for the environment of increasing power transmission capacity and the small underground space in urban area. The HTS cable (cold dielectric type) can flow four times larger electric current than the same sized traditional copper cable. Moreover, energy saving is more than the cooling cost of the HTS cable. In these reasons, many developed countries have been developing HTS cable. In Korea, over 10 years long term project to develop HTS cable system was launched in 2001 as one of the 21C Frontier R&D Program. The HTS cable being developed in Korea is cold dielectric type and has the specification of 154kV/1GVA.

Figure 1 shows the cross section of 154kV/1GVA HTS power cable. There are various types of heat load in the HTS cable such as AC loss in the HTS conductor, heat invasion through cryostat and heat loss in the various joints. Pressurized and subcooled liquid nitrogen (LN2) coolant flows through the core and the annuli to remove these heat generations and to maintain the temperature of HTS conductor below the vaporizing temperature but large pressure drops in the passages are inevitable due to the small hydraulic diameter. Thus the design of LN2 passage is the major factor which determines the cooling length.

Moreover, the mass flow rate of the coolant at each path should be balanced to keep minimum temperature rise along the cable length. Therefore the pressure drop characteristics should be identified.

* Corresponding author: jklee99@kyungnam.ac.kr

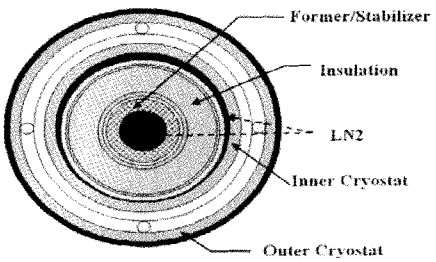

Fig. 1. 154 kV, 1GVA HTS Cable Cross Section.

Related with the shape of the coolant path, the former has spirally twisted shape due to the manufacturing process, and LN2 coolant flows through the hollow former core. Thus the passage in the core becomes the tube with spiral ribs. Also, the flow passage formed between inner cryostat and the HTS shield layer becomes annulus shape. Actually, the inner cryostat is corrugated pipe of stainless steel and its ratio of pitch to depth of corrugation is considered to be less than 5 to ensure flexibility as a power transmission cable. On the other hand, the HTS shield layer has smooth wall, thus the shape of the annulus become complex. Therefore, it should be needed the studies on the tubes with spiral ribs and the annuli, respectively.

Firstly, there are several previous studies on the development of pressure drop correlation for the single tubes with ribs and the corrugated tubes. For uniform-density, one-dimensional flow in a smooth tube the Fanning friction factor is defined as follows :

$$f \equiv \frac{D}{L}\frac{2\Delta P}{\rho V^2} \tag{1}$$

The friction factor concept has been extended to rough tubes when f is then a function also of surface roughness [1]. In turbulent flows inside a ribbed tube, the laminar sublayer is disturbed by the ribs, which increases the friction and thereby the pressure drop. Also, the pressure drop was increased because the boundary layer growth was suppressed by the generation of swirl flow due to the

repeated rib roughness for ribbed or spiral tubes. The augmented tube friction factor depends on the roughness height (e), pitch of roughness (p), helix angle of the roughness(α), and Reynolds number, among other variables. In normalized and non-dimensionalized form, the above relation, neglecting the minor effects such as profile shape, can be expressed as

$$f = fn(\mathrm{Re}, e/d, \alpha/90) \quad (2)$$

A survey friction factor studies for spirally fluted tubing was conducted by Bergles [2]. For laminar flow, a maximum increase in the friction factor of 200 percent was reported. For turbulent internal flow, the pressure drop was as much as 10 times higher than for plain tubes. Ravigururajan and Bergles [3] proposed generalized correlations for turbulent flow in several internally ribbed tube geometries. Jensen and Vlakancic [4] also suggested the correlation based on their adiabatic and diabatic water and ethylene glycol data for eight microfin.

The studies on the friction characteristics of annuli were difficult to find compared to those of the single tubes. Garimella and Christensen [5] studied on the annuli formed by placing a spirally fluted tube inside a smooth outer tube, but the present case is opposite shape, in other words, annuli with corrugated outer tube. They showed that the friction factor increases over smooth-annulus values were typically between 1.1 and 2.0 for laminar flow, and up to 10 for turbulent flow. And the annulus radius ratio is an important parameter in determining the fluted-annulus friction factor.

In this study, the experiments were performed to identify the pressure drop characteristics for core tubes (tubes with the ribs (microfins)) and for annuli with corrugated outer tube. And the previous pressure drop correlations were compared and assessed with the experimental results. Based on the analysis, the correlations for the present flow passages will be suggested.

2. EXPERIMENT

Test section

The test section specifications represented in Fig. 2 of the present cooling passage are summarized in Table 1. There are two types of tubes with ribs and eight types of annuli with two different outer diameters as shown in Fig.2 and 3, respectively.

TABLE I
SPECIFICATIONS OF TEST TUBES.

	Do(mm)	Di (mm)	p(mm)	e(mm)	α (deg)
Annulus	85.6	49,61	25.5	4.5	83
		68.7,70.5,72.4,73.7			
	108.7	77,90	28.5	4.5	83
Spirally grooved	12		5.3	0.8	72
	14		5.3	0.8	72

The cross section of the tube with ribs on axial flow direction and the passage flowing the test fluid are presented in Fig. 2(a) and (c), respectively. In Fig. 3, the 3D solid part represents the actual flow passage for annuli, and it can be checked that the inner wall is smooth and the outer wall is corrugated.

Experimental setup

A schematic diagram of the experimental setup is shown in Fig. 4. Water was used as the test fluid instead of the LN2 because of easy experiments. For identification of the heat transfer characteristics, the test fluid has to be replaced to LN2, and that will be future works. Water from the positive displacement pump flowed through calibrated flow meters and into the test section. A surge tank, located at a higher elevation and open to the atmosphere, was attached to the suction side of the pump.

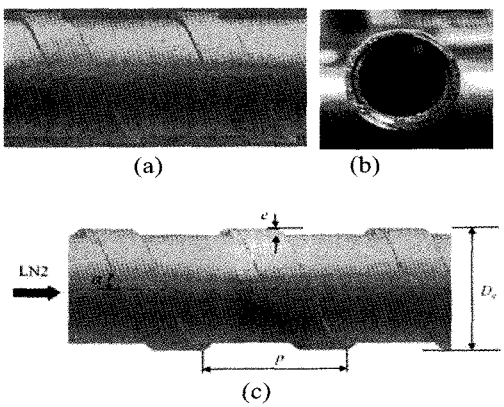

Fig. 2. Geometry of Core tube test section(Tube with spiral ribs).

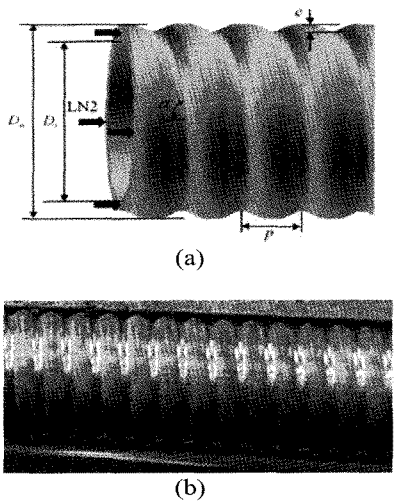

Fig. 3. Geometry of Annuli test section (Smooth inner wall and corrugated outer wall).

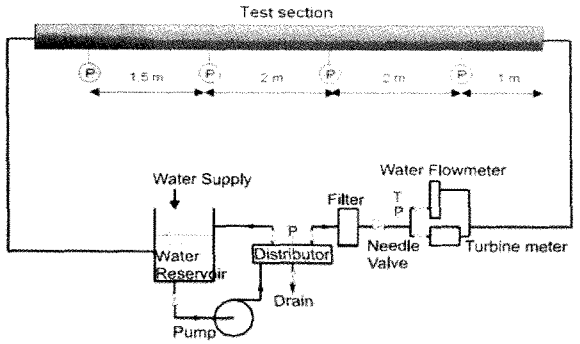

Fig. 4. Experimental Setup.

For the annuli pressure drop experiments, the three pressure tabs were installed circumferentially at each of four stations on the outer tube to obtain the average pressure value at the cross section of flow passage. And for the single tubes with spiral ribs, the pressure tabs were on the bottom at four stations. The pressure was measured by three differential pressure sensors and the data was stored by a data acquisition system consisting of a DAQ board (NI-SCXI) and a PC.

The uncertainties associated with the experimental data are calculated on the basis of a 95% confidence level as recommended by Moffat [6]. The analysis showed uncertainties of ±5.1% for the Reynolds number, 5% for pressure drop, and 6.1% for friction factor.

3. EXPERIMENTAL RESULTS

Friction factors for core tubes

For the core tube as shown in Fig.2, the experiments were performed with the range of Reynolds number 10^4 ~10^5, and the results are presented in Fig.5. The friction factor for smooth tube with the same hydraulic diameter as defined by Filonenko [7] is also presented.

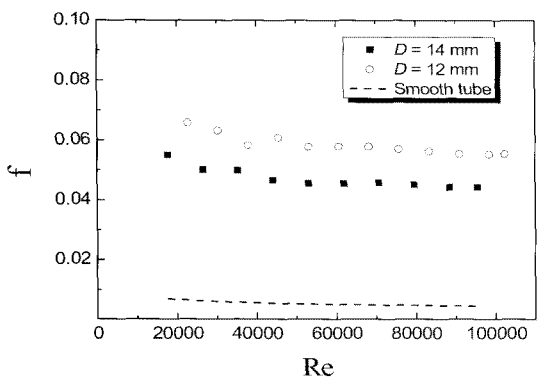

Fig. 5. Dependence of friction factor on the Reynolds number for ribbed tubes.

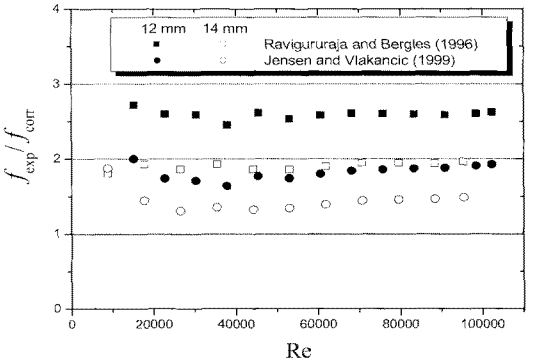

Fig. 6. Dependence of friction factor on the Reynolds number for ribbed tubes.

$$f_s = (1.58\ln \mathrm{Re} - 3.28)^{-2} \qquad (3)$$

The values for the friction factor of the present tubes are from 7 to 10 times higher than those of the smooth tubes. Also, the friction factor was increased as the surface roughness (e/d) increased as found in the previous studies.

For the present tubes, the pressure drop correlations by Ravigururaja and Bergles [3] and by Jensen and Vlakancic [4] that are known to be a good prediction from the previous results in eqs. (4) and (5), respectively.

$$\frac{f_{with\ ribs}}{f_s} = \{1+[29.1\ \mathrm{Re}^{a1}(\frac{h}{D})^{a2}(\frac{p}{D})^{a3}(\frac{\gamma}{90})^{a4}(1+1.47\cos\theta)]^{15/16}\}^{16/15}$$

(f_s in eq. (3))

Where,

$$a1 = 0.67 - 0.06p/d - 0.49\gamma/90,$$
$$a2 = 1.37 \setminus 0.157p/d,$$
$$a3 = -1.66\times10^{-6}\,\mathrm{Re} - 0.33\gamma/90,$$
$$a4 = 4.59 + 4.11\times10^{-6}\,\mathrm{Re} - 0.15p/d$$

$$\frac{f_{with\ ribs}}{f_s} = \left(\frac{l_c}{D}\right)^{-1.25}\left(\frac{A_n}{A}\right)^{1.75} - \frac{0.0151}{f_s}\times \left\{\left(\frac{l_c}{D}\right)^{-1.25}\left(\frac{A_n}{A}\right)^{1.75} - 1\right\}\exp\left(-\frac{\mathrm{Re}}{6780}\right) \qquad (4)$$

Where

$$\frac{l_c}{D} = 1 - 1.577\left(\frac{n\sin\gamma}{\pi}\right)^{0.64}\left(\frac{2h}{D}\right)^{0.53}\left\{\left(\frac{\pi}{n} - \frac{s}{D}\right)\cos\gamma\right\}^{0.28},$$

$$s = p/\cos\gamma - \frac{\pi}{4}\left(D^2 - D_e{}^2\right)/nh \tag{5}$$

Figure 6 shows the comparison results between those correlations and the present data. The experimental results were higher than the prediction values. This may be the shape of the fins on the tube surface. In other words, the area of the fins was very small compared to that of the flow path and the height and the width of the fins were not much different. But in this case, the width of the fins was very large, thus the space between the fins was small as shown in Fig. 2. That makes the cross-area smaller, thus the pressure drop would increase. But the tendency will be identified in the future works.

Among the correlations, the model by Jensen and Vlakancic [4] was better, thus the equation was modified. The exponents were correlated by the experimental database, thus a statistical approach was used by applying the present results to the model and minimizing the least square differences in the dependent variables. The most effective model was found to be

$$\frac{f_{with\ ribs}}{f_s} = \left(\frac{l_c}{D}\right)^{-1.65}\left(\frac{A_n}{A}\right)^{2.15} - \frac{0.0151}{f_s}\times \left\{\left(\frac{l_c}{D}\right)^{-1.65}\left(\frac{A_n}{A}\right)^{2.15} - 1\right\}\exp\left(-\frac{\mathrm{Re}}{6780}\right)$$

Where

$$\frac{l_c}{D} = 1 - 1.577\left(\frac{n\sin\gamma}{\pi}\right)^{0.64}\left(\frac{2h}{D}\right)^{0.53}\left\{\left(\frac{\pi}{n} - \frac{s}{D}\right)\cos\gamma\right\}^{0.28}$$

$$, \; s = p/\cos\gamma - \frac{\pi}{4}\left(D^2 - D_e{}^2\right)/nh \tag{6}$$

It can be predicted within the range of 10 % as shown in Fig. 7.

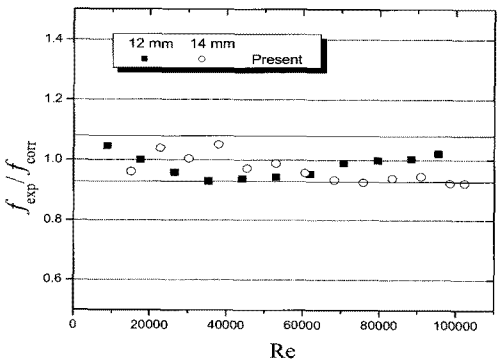

Fig. 7. Comparison results between the modified models and experimental results for core tube.

Friction factors for annuli

The friction factors for 8 cases annuli (2 corrugated tube types for outer tube and 6 smooth tube types for inner tube as listed in Table 1 and as shown in Fig. 3) were shown in Fig. 8 with the range of Reynolds number 3000 ~ 10^4. The values are decreased with higher Reynolds number, and that can be found in the previous studies. And the friction is increased with the smaller gab between the inner and the outer tube. The similar annuli shape that consists of the corrugated surface for outer part and the smooth surface for inner part was not able to find in previous studies. Therefore, the applicability of the previous pressure drop model for annuli was identified, and if needed, the model to predict would be suggested.

Kakac et al. [8] suggested the following correlation that is applicable for turbulent flow in smooth annuli:

$$f_s = 4\left[1.7372\left(\frac{\mathrm{Re}}{1.964\ln\mathrm{Re} - 3.8215}\right)\right]^{-2}(1 + 0.0925r^*) \tag{7}$$

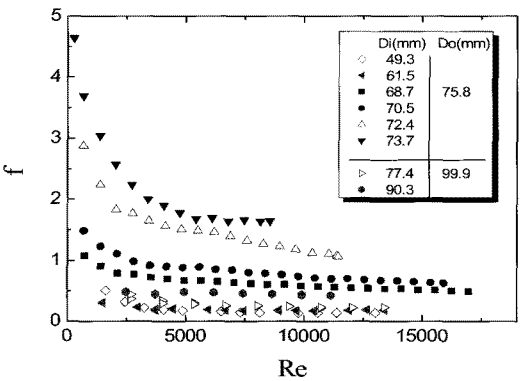

Fig. 8. Dependence of friction factor on the Reynolds number for annulus.

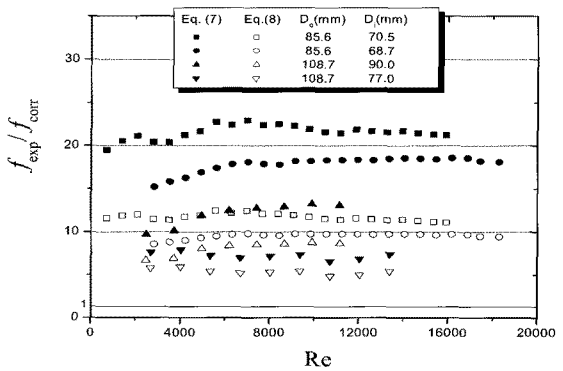

Fig. 9. Comparison results between the previous and experimental results.

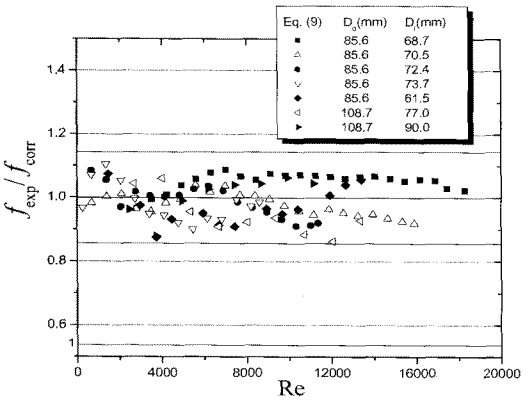

Fig. 10. Comparison results between the modified models and experimental results for core tube.

The pressure drop is related with Reynolds number and the annulus radius ratio. Garimella and Christensen [5] modified the above correlation with the enhancement function (ef) for the annuli formed by placing a spirally fluted tube inside a smooth outer tube.

$$f_f = f_s\, e_f \quad \text{Where}$$

$$e_f = (1 + 222\,\mathrm{Re}^{0.09}\, e^{*2.40}\, p^{*-0.49}\theta^{-0.38} r^{*2.22}) \qquad (8)$$

Eqs. (7) and (8) were applied to measured values, and the results are presented in Fig. 9. The friction factors are higher than those of the smooth annuli about 20 ~ 30 times. This is because flow blockage due to area reduction and the rotational flow produced by the spiral ridge make the pressure drop larger. Also, friction factors for the annuli with spirally fluted tube inside a smooth outer tube are about 5 to 10 times. It may be the more strong rotational flow due to the outer corrugation compared to that generated from inner fluted tube. Moreover, because the ratios of the maximum distance from inner wall to outer corrugated wall (D_o-D_i+e) divided by the minimum (D_o−D_i−e) are very large, the turbulent effects should be enhanced by sudden flow path area change. But that must be checked by identification of the flow field from experiments or flow field calculations in the future work.

Therefore, the pressure drop correlation for the present shape of the annuli was derived. The enhancement factor in Eq. (8) was modified, and that can be found to be :

$$e_f = (1.43 + 9.06\cdot 10^{-12}\cdot \exp(r^*/0.034) + 3050\,\mathrm{Re}^{0.09}\, e^{*2.40}\, p^{*-0.49}\theta^{-0.38} r^{*2.22}) \qquad (9)$$

It can be predicted within the range of 15 % as shown in Fig. 10.

4. CONCLUSION

The experiments were performed to identify the pressure drop characteristics for core tubes (tubes with the ribs (microfins)) and for annuli with corrugated outer tube. The pressure drops in the core tubes and the annuli are much higher than the tubes with smooth surface. And the previous pressure drop correlations were compared but the results were not good. Therefore the correlations to predict the pressure drop in each tube were suggested.

ACKNOWLEDGMENT

This research was supported by a grant from Center for Applied Superconductivity Technology of the 21st Century Frontier R&D Program funded by the Ministry of Education, Science and Technology, Republic of Korea.

REFERENCES

[1] Moody, LF., An approximate formula for pipe friction factors, Mech Engng., 69, pp. 1005–6, 1947.
[2] Bergles, A. E., Heat transfer characteristics of Turbotec Tubing, Heat Transfer Lab. Report HTL-24 ISU-ERI-Ames-81018, Iowa State Univ., 1980.
[3] Ravigururajan TS, Bergles AE., General correlations for pressure drop and heat transfer for single-phase turbulent flow in internally ribbed tubes, Augmentation of Heat Transfer in Energy Systems, ASME-HTD, 52, pp. 9– 20, 1985.
[4] Jensen MK, Vlakancic A., Experimental investigation of turbulent heat transfer and fluid flow in internally finned tubes. Int. J. Heat Mass Transfer, 42, pp. 1343–51, 1999.
[5] Garimella and Christensen, Heat Transfer and Pressure Drop Characteristics of Spirally Fluted Annuli: Part I—Hydrodynamics, Transactions of the ASME, J. Heat Transfer, 117, pp. 54-60, 1995.
[6] Moffat, R. J., Describing the Uncertainties in Experimental Results, Exp. Fluid Thermal Sci., 1, pp. 3-17, 1988.
[7] Filonenko, G. K., Hydraulic Resistance in Pipes, Teploergetica1, 4, pp. 40-44, 1954.
[8] Kakac, S., Shah, R. K., and Aung, W., Handbook of Single-Phase Convective Heat Transfer, Wiley, New York, 3-92 and 4-132, 1987.